Acta Polytechnica CTU Proceedings **55**:41–48, 2025
https://doi.org/10.14311/APP.2025.55.0041

Published by the Czech Technical University in Prague

MICROSTRUCTURAL AND MECHANICAL PROPERTY CHARACTERIZATION OF HIGH-DENSITY URANIUM FUEL FOR LIGHT-WATER REACTORS

Filip Mach[a,*], Patricie Halodová[b], Martin Ševeček[a], Jakub Krejčí[c], Petr Šárek[c]

[a] *Czech Technical University in Prague, Faculty of Nuclear Sciences and Physical Engineering, Department of Nuclear Reactors, V Holešovičkách 2, 180 00 Prague 8, Czech Republic*

[b] *Research Centre Řež s.r.o., Hlavní 130, 250 68 Husinec – Řež, Czech Republic*

[c] *UJP PRAHA a.s., Nad Kamínkou 1345, 156 00 Prague – Zbraslav, Czech Republic*

[*] corresponding author: machfil1@cvut.cz

Abstract. One of the key concepts in the development of accident-tolerant fuels (ATFs) involves the use of high-density fuels, aimed at improving the safety and economics of light-water reactors. This work focuses on the microstructural and mechanical characterization of experimentally fabricated segments of dispersion-type high-density uranium fuels with a zirconium matrix and Zr-based cladding, intended for future testing in research reactors. Both U-Mo alloys and pure uranium metal were investigated, with particular attention given to the influence of thermal treatment on the phase composition and microstructure of the fuel segments. In addition, changes resulting from thermal exposure were evaluated. The research includes the identification of newly formed phases during transient conditions and the analysis of diffusion phenomena in the material. Mechanical properties were evaluated through microhardness measurements, and the results will serve as input parameters for computational simulations using the Serpent code to support the introduction of these fuels in the VR-2 research reactor.

Keywords: Accident tolerant fuels, high-density uranium fuels, microstructure, research reactor, U-Mo.

1. Introduction

The pursuit of improved safety and efficiency in nuclear reactors has driven the development of alternative fuel concepts with improved performance under normal and accident conditions. Among these, high-density fuels (HDFs) have emerged as promising candidates as a result of their potential to increase the concentration of fissile atoms, extend fuel cycles, and ensure better heat dissipation from the fuel, leading to its lower maximum temperatures. Their implementation is particularly relevant in the context of accident-tolerant fuels (ATFs), which are designed to withstand severe conditions for much longer times compared to traditional Zr+UO_2 fuel systems [1, 2].

Traditional UO_2-based fuels, while well understood and widely deployed, face limitations in terms of thermal conductivity and structural resilience under high-temperature or off-normal scenarios. In contrast, HDFs – including uranium alloys, silicides, carbides, and nitrides – offer improved thermophysical properties, such as a higher uranium fissile density and superior thermal conductivity. These properties can enable longer operational cycles and improved tolerance to transients and accidents [3, 4].

This research investigates selected high-density fuel types suitable for power reactors, with a particular focus on uranium-based metal compounds. The study combines experimental characterization of the microstructure and composition of the fuel with numerical simulations to assess the interaction of the fuel with neutrons. The results contribute to the larger effort to qualify advanced nuclear fuels that meet the performance and safety demands of modern nuclear systems.

2. Materials and methods

2.1. Fuel sample preparation

All high-density fuel (HDF) samples analyzed in this study were provided by UJP PRAHA as part of a collaborative project with Centrum výzkumu Řež (CVŘ) and Czech Technical University in Prague (CTU) within the CANUT-II programme. The production process followed the methodology established in a previous Master's thesis and involved two main stages: mechanical compaction and thermal impregnation [5].

The fuel elements consisted of metallic uranium fragments (0.2–3.8 in diameter) combined with matrix materials based on zirconium, copper, and iron alloys. The mixture was vibrationally compacted into cladding tubes in three stages, achieving approximate volume fractions of 44 % fuel, 12 % matrix, and 44 % porosity. After compaction, the samples were hermetically sealed, and one of the samples (HDF-U-2) was

filled with argon at 0.2 MPa prior to closure. The final densification and microstructural homogenization were achieved by heat treatment at 900 °C, followed by cooling with argon. To relieve residual stresses and prevent structural damage to the cladding, vacuum annealing was performed at 575 °C for 180 minutes [5].

Furthermore, a sample was subjected to a thermal ramp scenario with heating to 1000 °C and rapid quenching in ice water to assess the resistance to thermal shock [5].

2.2. Stabilization of γ-U phase by Mo

At room temperature, uranium crystallizes in the orthorhombic α phase, which is stable up to 668 °C. Although thermodynamically favorable, this phase exhibits poor mechanical properties, such as brittleness and dimensional instability, due to its anisotropic crystal structure [6].

Alloying uranium with molybdenum stabilizes the high-temperature γ-phase (bcc), which is otherwise stable only above 774 °C. Molybdenum suppresses the $\gamma \rightarrow \alpha$ transformation during cooling and promotes retention of the γ phase at room temperature. Alloys containing 7–10 % Mo typically retain this structure, improving ductility, dimensional stability, and irradiation tolerance [6, 7].

2.3. Sample preparation and metallography

All samples were embedded in epoxy resin, ground, and polished using standard metallographic procedures [5]. Optical microscopy was performed using a Nikon Eclipse LV100N POL microscope. Image analysis (component fraction and grain size) was performed using the FIJI software.

2.4. Scanning electron microscopy and EDX

Microstructural and compositional analyzes were conducted using a Tescan MIRA 3 GMU scanning electron microscope (SEM) equipped with a field emission gun and an Oxford Instruments Energy Dispersive Spectrometer (EDX). Before SEM analysis, all samples were coated with carbon to prevent charging. Measurements included BSE imaging and EDX point analysis, line scans, and acquisition of elemental maps to assess uranium fragments and matrix composition, and interfacial interactions.

2.5. Scanning electron microscopy – EBSD

Electron Backscatter Diffraction (EBSD) analysis was performed on the Tescan MIRA 3 GMU SEM system and using the same Oxford Instruments software. The samples were mechanically polished on vibratory polishing with colloidal silica to ensure a high-quality, deformation-free surface. EBSD was used to obtain the phase composition of the uranium fragments. Data processing included noise reduction and cleanup procedures to improve pattern indexing and reliability.

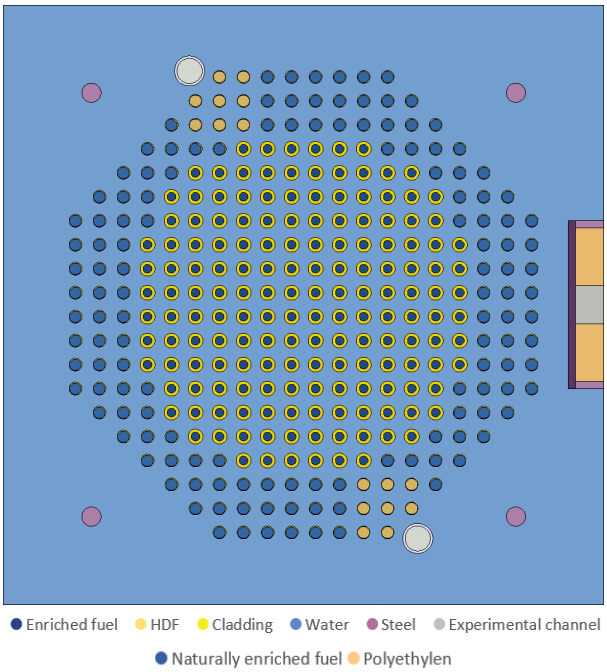

Figure 1. Top view of the center and nuclear reactor core of VR-2 with replaced fuel rods near two experimental channels.

2.6. X-Ray Diffraction (XRD)

Phase composition was evaluated using a 4 kW powder X-ray diffractometer with a Co anode. Samples were trimmed to < 1 cm thickness and mounted for reflection mode analysis. Scans were performed in areas of high concentrations of fuel and matrix.

2.7. Nanoindentation

Local mechanical properties were measured using a Hysitron Ti 950 TriboIndenter equipped with a Berkovich tip. Hardness and modulus were determined on the basis of load-displacement data using the Oliver and Pharr method. Indentations were performed at multiple points in the fuel and matrix regions.

3. Neutronic simulations

The neutron-physical behavior of the HD fuel was evaluated using the Serpent Monte Carlo code (version 2.1.32). All calculations used nuclear data from ENDF/B-VIII.0. The simulations were based on a modified core configuration of the VR-2 reactor at CTU in the external source mode (^{252}Cf), with selected fuel rods replaced by HDF elements (Figure 1). VR-2 is a subcritical reactor used for teaching purposes [8].

The VR-2 core contains two fuel types: EK-10 rods in the central region, made of a UO_2-Mg alloy with 10 % enrichment and aluminium cladding, and

Sample	Fuel [%]	Matrix [%]	Porosity [%]	Mean Fragment Area [mm^2]
HDF-U-1	44.8	31.3	23.9	3.18
HDF-UMo	47.2	26.1	26.7	2.37
HDF-U-2	26.2	18.7	55.1	2.16

TABLE 1. Volume fractions and average fuel fragment size from LOM image analysis.

peripheral rods of natural metallic uranium also with aluminium cladding.

There are two experimental channels, Channel 1 and Channel 2, placed symmetrically near the central region. As shown in Figure 1, up to eight fuel rods located closest to the experimental channels were replaced, in separate scenarios, with HDF materials of varying enrichment. This location was chosen because proximity to the channels makes changes in neutron-flux density easier to measure. Material compositions obtained from the experimental characterization were used as input for the high-density fuel rods.

Two fuel configurations were considered in the calculations: a homogenized model and a layer model, which represents a fuel with dispersed particles. The homogenized model contained fuel, matrix, and pores in which argon was considered at a pressure of 0.2 MPa, corresponding to the conditions used during the encapsulation of the sample. The effective density was calculated for the new homogeneous material. In the layered model, the fuel was considered in the middle of the rod, and a homogenized matrix with pores was located around it.

These simulations aim to assess the impact of the microstructural fuel configuration on local relative neutron flux density in experimental channels and to find a configuration that will produce a measurable change in neutron flux density and that will contain as few fuel rods with as little enrichment as possible.

4. RESULTS

Three fuel samples HDF-U-1, HDF-UMo, and HDF-U-2 were prepared and analyzed using light optical microscopy (LOM), scanning electron microscopy (SEM) with energy-dispersive X-ray spectroscopy (EDX) and nanoindentation. The fuel matrices' expected composition is zirconium-based alloy (Zr 83.8 %, Cu 8.1 %, Fe 8.1 %), with uranium or uranium–molybdenum fragments embedded inside. The estimated uranium content per sample was approximately 1.6 g.

4.1. QUANTITATIVE MICROSTRUCTURAL ANALYSIS

LOM-based image analysis quantified the volumetric distribution of fuel fragments, matrix, and porosity (Table 1). The sample HDF-U-2 (Figure 2), subjected to high temperature ramp, showed the highest porosity (55.1 %) and the lowest fuel content (26.2 %). In contrast, HDF-UMo (U-9Mo) showed the highest fuel content (47.2 %) and relatively low porosity (26.7 %). All of these data may be affected by the evaluation method in ImageJ. The error estimate was conservatively estimated to be 1 %.

FIGURE 2. Light optical microscopy image of HDF-U-2.

4.2. SEM/EDX CHARACTERIZATION

SEM-BSE images and EDX line scans revealed interdiffusion phenomena between the fuel, matrix, and cladding. In both samples based on U and U-9Mo, the diffusion of uranium into the zirconium alloy matrix was confirmed. In the HDF-UMo sample, a Mo boundary zone was observed between the fuel and the matrix (Figure 3). Uranium was also detected at low levels in the cladding, attributed to sample preparation artifacts.

The HDF-UMo matrix showed a granular morphology, with zirconium encased in iron, and local segregation of elements. In HDF-U-1, the penetration of uranium into the matrix resulted in needle-shaped structures where uranium localized replaced Cu and Zr; Fe was also present in these areas (Figure 4). The uranium content decreased sharply at the matrix-cladding interface (Figure 5).

The HDF-U-2 sample exposed to elevated temperatures exhibited extensive cracking and disintegration of the fuel. Uranium was found to be widely distributed throughout the matrix and partially migrated into the cladding (Figure 6). The structural transformation of the matrix was observed, from needle-shaped to elongated grains interspersed with uranium dendrites (Figure 7b). A secondary matrix phase

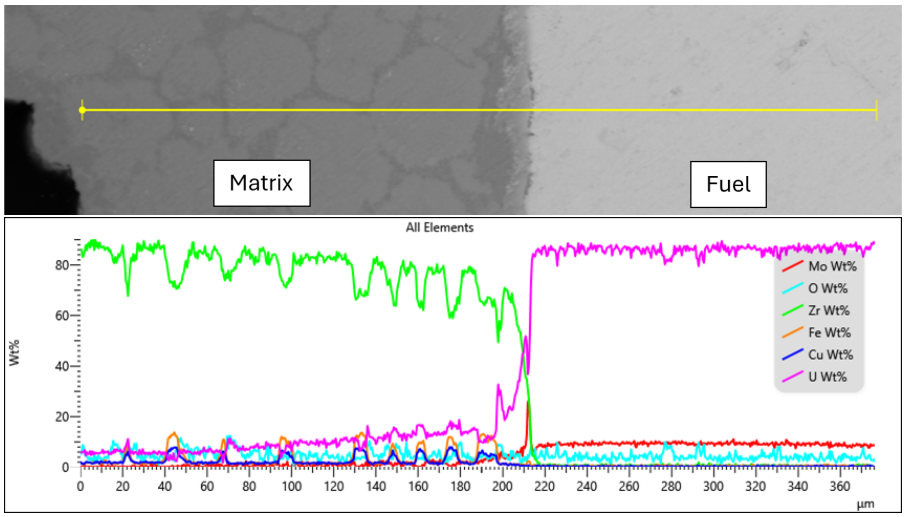

Figure 3. EDX line scan of sample HDF-UMo at the fuel–matrix interface, showing the formation of a contact zone and element gradients.

Sample	Component	E [GPa]	σ_E [GPa]	H [GPa]	σ_H [GPa]
HDF-U-1		124.3	10.2	7.6	1.2
HDF-U-2	Fuel	131.1	15.3	7.3	1.4
HDF-UMo		108.0	9.3	6.2	0.9
HDF-U-1		166.3	9.1	6.7	0.7
HDF-U-2	Matrix	166.3	12.4	7.3	1.2
HDF-UMo		110.0	14.0	6.8	1.9

Table 2. Average values of Young's modulus (E) and hardness (H) obtained by nanoindentation for three high-density fuel variants.

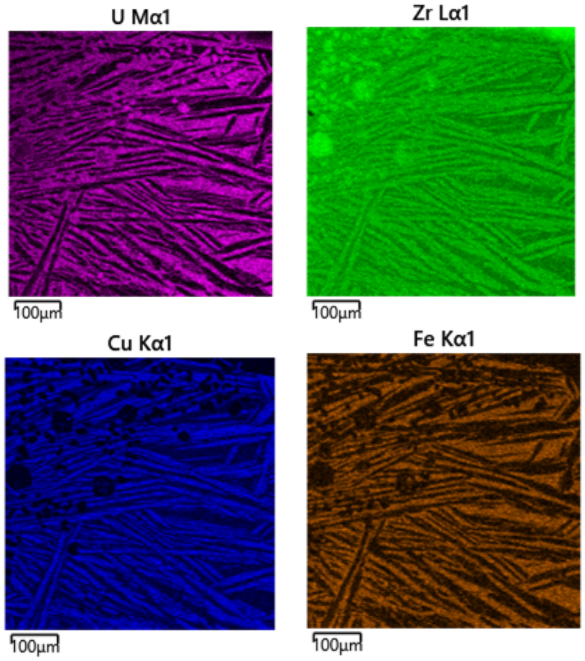

Figure 4. EDX elemental map of U, Zr, Cu and Fe in the matrix region near a fuel fragment in HDF-U-1.

containing Fe and a minor Zr was formed at the fuel–matrix interface.

These microstructural alterations suggest that elevated temperature conditions significantly accelerate uranium diffusion and potentially compromise the cladding integrity due to enhanced fuel–matrix–cladding interactions. The interaction between the matrix and the cladding can be seen in Figure 8.

4.3. Mechanical testing

Nanoindentation was performed both in the fuel fragment region and in the matrix. The results showed that the HDF-UMo alloy exhibits the lowest elastic modulus and hardness, which is consistent with the expected microstructural change caused by molybdenum alloying. The sample exposed to elevated temperature does not exhibit a significant decrease in hardness or modulus, indicating good mechanical stability after thermal shock.

The average values of Young's modulus and hardness, including standard deviations, are given in Table 2.

4.4. XRD phase identification

XRD was performed to characterize the crystalline phases and corroborate the elemental analysis based

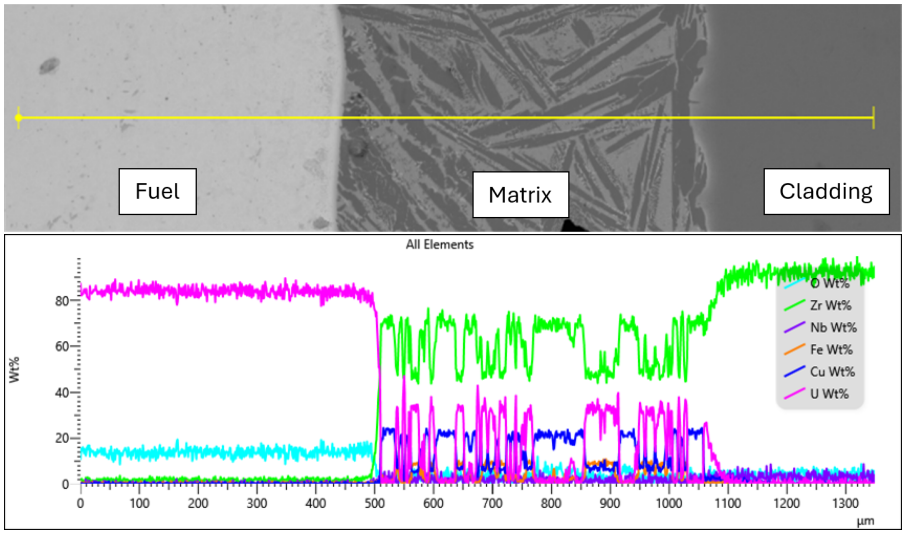

FIGURE 5. EDX line scan of HDF-U-1 across fuel, matrix, and cladding, showing uranium distribution gradient.

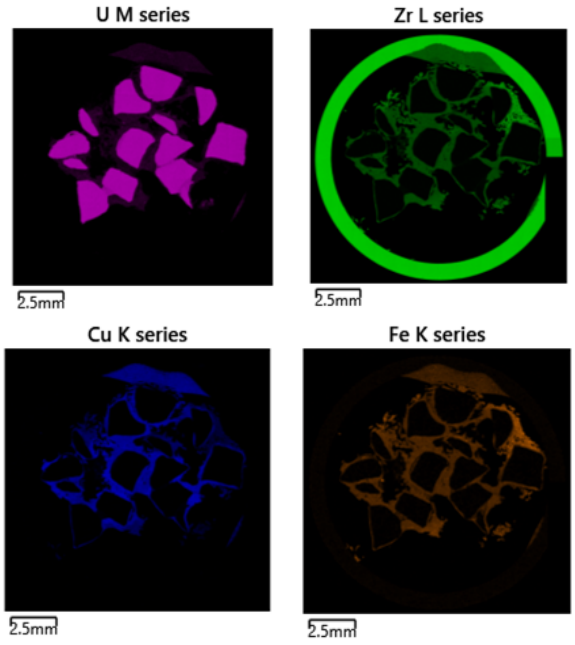

FIGURE 6. EDX elemental distribution map of sample HDF-U-2 after exposure to elevated temperature.

on EDX. Each of the three samples showed distinct features, particularly in the fuel and matrix regions.

HDF-U-1: The diffraction pattern confirmed the presence of uranium in the α-U phase. Both the fuel and matrix regions showed signs of surface oxidation. In the matrix, zirconium and iron were detected. However, given the EDX data, where Zr and Fe appear in separate needle-shaped regions, the joint detection in XRD likely reflects the lower spatial resolution of this technique. Copper, though expected in a concentration higher than that of iron per EDX, was less prominent, probably because of its colocalization with more strongly diffracting zirconium.

HDF-UMo: The fuel exhibited uranium in the stabilized γ phase, consistent with the presence of

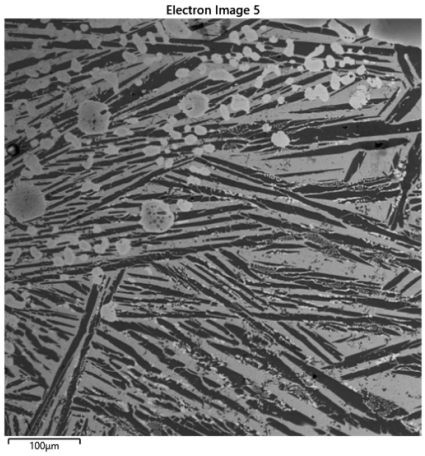

(A). Microstructure of the matrix in HDF-U-1; needle-like morphology.

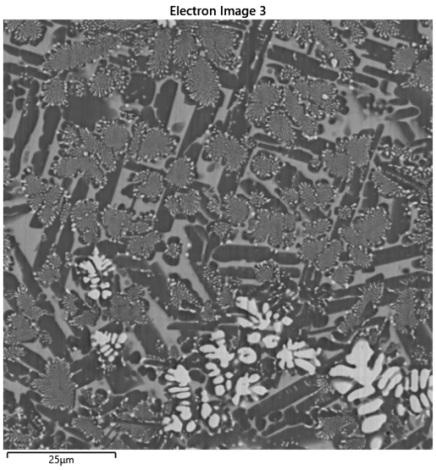

(B). Microstructural change of the matrix in HDF-U-2 due to thermal exposure: transition from needle-like to elongated grain morphology with dissipated uranium fragments.

FIGURE 7. Microstructure of the matrix in HDF-U-1 and HDF-U-2 obtained by Scanning Electron Microscopy (SEM) Backscattered Electrons (BSE).

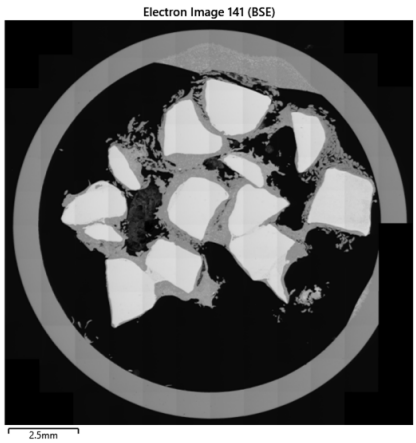

Figure 8. Interaction of the matrix with cladding in HDF-U-2.

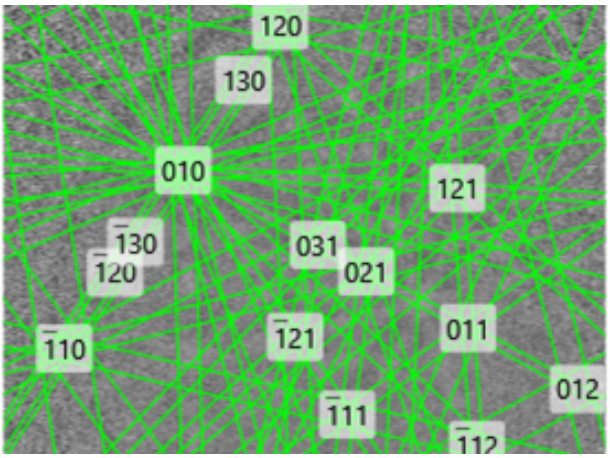

Figure 9. EBSD analysis in matrix of sample HDF-U-2.

molybdenum. This confirms Mo's role in phase stabilization. Uranium diffusion into the matrix was limited, as evidenced by both EDX and XRD. Consequently, iron and copper peaks were more clearly observed in the matrix, being less masked by uranium.

HDF-U-2 (exposed to elevated temperature): Surprisingly, the XRD patterns of the fuel did not significantly deviate from those of HDF-U-1, despite the thermal exposure. In the matrix, copper signals were more prominent than in other samples. This is consistent with EDX mapping, which showed increased uranium diffusion overshadowing the iron signal. In contrast to non-heated samples, certain matrix regions exhibited higher copper content than zirconium, allowing improved detection of Cu-related diffraction peaks.

These findings indicate that thermal exposure affects the matrix element visibility in XRD mainly via uranium redistribution. While fuel phase composition remained relatively stable, matrix heterogeneity increased.

4.5. SEM/EBSD characterization

Electron backscatter diffraction (EBSD) analysis was performed to complement the structural and phase characterization. Successful diffraction patterns were obtained predominantly within the matrix regions of all samples. The results confirmed the presence of expected crystalline phases corresponding to the constituent elements of the zirconium-based alloy – namely α-Zr (Figure 9).

In contrast, diffraction within the fuel regions was largely unsuccessful due to poor pattern quality and possible surface oxidation, except for one localized area in the HDF-UMo sample (Figure 10). In this region, a well-indexed EBSD pattern confirmed the presence of the stabilized γ-U phase, supporting the XRD and compositional findings. This result provides further evidence of the successful stabilization of the high-temperature uranium phase by molybdenum addition.

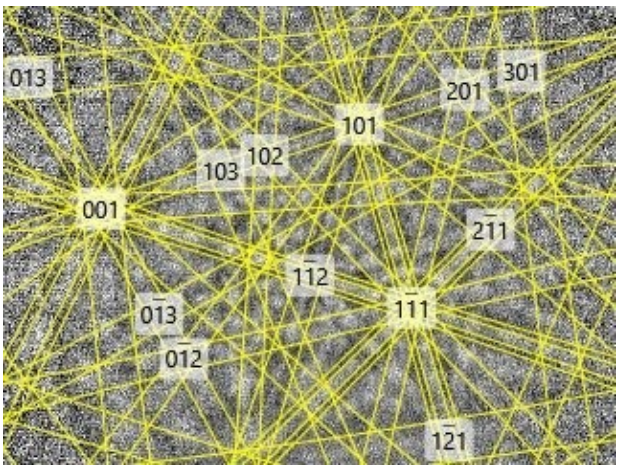

Figure 10. EBSD analysis of a sample HDF-UMo in fuel.

4.6. Neutronic simulations

The reference configuration represents the unmodified core with all rods containing standard fuel. Relative neutron flux densities in both channels were extracted and normalized to this reference.

First, six simulations were performed for configurations with 8 replaced rods with homogenized fuel U and U-Mo with enrichments of 0.72, 1.5 and 4.0 %. From these values, an enrichment value was determined for which the measured neutron flux densities in the experimental channels should differ from the reference values by at least 10 %. Such a change should already be realistically detectable.

This value was set at an enrichment of 1.73 % for molybdenum fuel and 1.77 % for uranium fuel.

The fuel layer with the same composition showed slightly reduced neutron flux densities in the range of 0–2 % with a direct proportionality depending on the enrichment. Therefore, only homogenized fuel was further simulated, since the results do not differ much and the real measured values of neutron flux will be approximately in between the values of layered and homogenized fuel.

8 Rods	**Channel1** [%]	**Channel2** [%]
UMo 0.72 %	-4.87	-5.57
UMo 1.50 %	8.39	7.25
UMo 4.00 %	47.16	36.48
U 0.72 %	-10.04	-4.15
U 1.50 %	10.91	9.76
U 4.00 %	51.87	40.69
5 Rods		
UMo 2.20 %	7.60	9.08
UMo 2.60 %	15.37	14.14
U 2.20 %	13.67	8.66
U 2.60 %	17.28	16.79

TABLE 3. Percentage change in neutron flux density in experimental channels relative to the reference nuclear reactor core configuration. The relative deviation was below 2 % for all calculations. Only for calculations with an enrichment of 2.2 % was the deviation on the detectors slightly higher than 3 %.

Based on these results, further simulations were conducted for configurations with five replaced rods closest to the experimental channels. Two simulations were performed for each U and U-Mo fuel, and the enrichment at which the simulated neutron flux differs from the reference by at least 10 % was derived from simulations to 2.30 % for U-Mo and 2.12 % for U. All results are summarized in Table 3.

5. Discussion

The results obtained in this study show that the neutronic performance of pure uranium and U-Mo fuels dispersed in zirconium-based matrices is significantly lower compared to conventional fuels based on naturally enriched uranium. This observation is in agreement with the findings of Keiser et al. [6], who reported a noticeable penalty in reactivity when using dispersed high-density LEU fuels due to their reduced fraction of the uranium volume, especially compared to the U-Al fuel used in reactor VR-2.

The inferior neutronic behavior observed here is primarily related to the limited uranium loading achievable in the tested fuel geometry. Similar conclusions were drawn by Savchenko et al. [7], who noted that although monolithic U-Mo fuels exhibit high uranium densities, the introduction of a matrix or dispersion significantly dilutes the fissile content, thus reducing the macroscopic fission cross section.

Furthermore, the practical deployability of these novel fuel types must consider not only their reactivity but also their manufacturability and long-term stability. Savchenko et al. [9] emphasize that U-Mo systems require advanced fabrication routes and face issues related to fuel/matrix interaction, swelling, and phase transformations under irradiation. Our findings confirm that even in simplified models, U-Mo-dispersed fuels may not meet the performance requirements of existing reactors without significant redesign of core parameters.

Lastly, while high-density fuels remain promising from a nonproliferation perspective, their implementation in nuclear reactors is limited by tight margins in reactivity and licensing constraints. Therefore, standard fuels with proven performance, such as naturally enriched UO_2, currently remain the most viable option for nuclear reactors.

6. Conclusions

This study presents an integrated experimental and simulation-based evaluation of dispersion-type high-density uranium fuels intended for light-water reactor applications. Three fuel variants, based on pure uranium and uranium-molybdenum alloy, were characterized in terms of microstructure, composition, mechanical behavior, and neutronic performance.

The key conclusions are as follows:

- Microstructural analysis revealed strong thermal sensitivity, and the pure uranium sample was subjected to higher temperature conditions, exhibiting cracking, increased porosity, and extensive uranium redistribution.
- XRD and EBSD phase identification confirmed stabilization of α-U in pure uranium and γ-U in U-Mo fuel, supporting the beneficial effect of molybdenum on phase stability and suppression of diffusion.
- Mechanical testing showed that U-Mo samples had lower hardness and modulus, indicating higher ductility. The thermally ramped sample maintained acceptable mechanical performance, but compromised the integrity of the cladding due to the matrix-cladding interaction and the reduction in the thickness of the cladding.
- Neutronic simulations demonstrated that strategic replacement of standard rods with HDF variants leads to detectable increases in local neutron flux near experimental channels, although a higher enrichment is required. At least 1.7 % enrichment is sufficient to cause > 10 % changes in flux density, offering a viable path for experimental fuel testing under controlled neutronic conditions.

These findings suggest that these dispersed high-density fuels can be fabricated and used for experimental purposes in reactor VR-2, although higher enrichment or an optimized internal configuration with increased uranium loading would be required to achieve comparable neutronic performance.

Acknowledgements

We acknowledge the state support of the Technology Agency of the Czech Republic within the National Competence Centre Programme II, project TN02000012 „Center of Advanced Nuclear Technology II“. The presented results were obtained using the CICRR infrastructure, which is financially supported by the Ministry of Education, Youth and Sports – project LM2023041.

References

[1] Nuclear Energy Agency. *State-of-the-Art Report on Light Water Reactor Accident-Tolerant Fuels*. Nuclear Science. OECD Publishing, Paris, 2018. https://doi.org/10.1787/9789264308343-en

[2] G. Youinou, R. S. Sen. Enhanced accident tolerant fuels for LWRs – A preliminary systems analysis. Tech. rep., Idaho National Laboratory (INL), Idaho Falls, ID (United States), 2013. https://doi.org/10.2172/1111499

[3] I. I. Konovalov, Y. S. Stetsky. Development status of metallic, dispersion and non-oxide advanced and alternative fuels for power and research reactors. IAEA-TECDOC 1374, International Atomic Energy Agency, Vienna, Austria, 2003.

[4] K. A. Gamble, J. D. Hales, G. Pastore, et al. Behavior of U_3Si_2 fuel and FeCrAl cladding under normal operating and accident reactor conditions. Tech. rep., Idaho National Laboratory (INL), Idaho Falls, ID (United States), 2016. https://doi.org/10.2172/1364507

[5] M. Přibyl. *Vysokohustotní palivo pro jaderné reaktory [In Czech; High Density Fuel for Nuclear Reactors]*. Master's thesis, CTU in Prague, Faculty of Nuclear Sciences and Physical Engineering, 2022. [2025-07-10]. http://hdl.handle.net/10467/105390

[6] D. D. Keiser, S. L. Hayes, M. K. Meyer, C. R. Clark. High-density, low-enriched uranium fuel for nuclear research reactors. *JOM* **55**(9):55–58, 2003. https://doi.org/10.1007/s11837-003-0031-0

[7] A. M. Savchenko, L. A. Karpyuk, E. A. Dergunova, et al. Fuel cycles with advanced dispersion fuel elements of high uranium density. *Atomic Energy* **134**:181–189, 2023. https://doi.org/10.1007/s10512-024-01041-7

[8] J. Rataj, F. Fejt, J. Frýbort, et al. The project of VR-2 subcritical assembly. *Nuclear Engineering and Design* **386**:111578, 2022. https://doi.org/10.1016/j.nucengdes.2021.111578

[9] A. Savchenko, A. Vatulin, I. Konovalov, et al. Fuel of novel generation for PWR and as alternative to MOX fuel. *Energy Conversion and Management* **51**(9):1826–1833, 2010. 14th International Conference on Emerging Nuclear Systems (ICENES 2009). https://doi.org/10.1016/j.enconman.2010.01.027